

## Black blood MRI of the carotid arteries with local excitation coils at 7 tesla

Tijl A. van der Velden<sup>1</sup>, Wouter Koning<sup>1</sup>, Maarten J. Versluis<sup>2</sup>, Dennis W.J. Klomp<sup>1</sup>, Peter R. Luijten<sup>1</sup>, and Jaco J.M. Zwanenburg<sup>1</sup>

<sup>1</sup>Radiology, University Medical Center Utrecht, Utrecht, Utrecht, Netherlands, <sup>2</sup>Radiology, Leiden University Medical Center, Leiden, Zuid-Holland, Netherlands

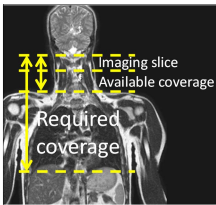


Figure 1: Required coverage of standard blood suppression techniques and available coverage at 7T

**Introduction:** Rupturing plaques in the carotid arteries are associated with cerebrovascular stroke. MRI can be used to study plaque composition, which is needed to assess the risk of plaque ruptures. High field (7T) MRI may improve assessment of plaque composition, due to the higher intrinsic SNR. A dedicated transmit coil with separate receive array has been built for this application [1]. However, the big challenge of *blood signal suppression* remains. Conventionally used blood suppression techniques like dual inversion recovery (DIR) and quadruple inversion recovery (QIR) require a large blood preparation slab (see fig. 1). The local excitation coils at 7T do not have sufficient coverage. For robust blood suppression typically spin echo based sequences (intrinsic blood signal suppression) are used at 7T, making the high  $T_1$  contrast in plaque imaging that is generally provided with

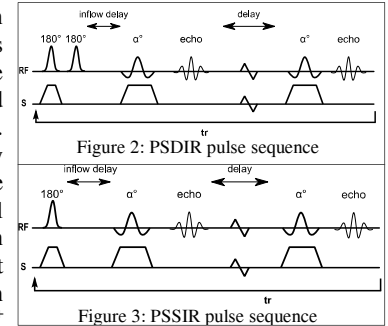


Figure 2: PSDIR pulse sequence

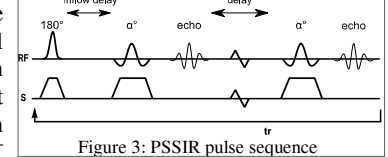


Figure 3: PSSIR pulse sequence

gradient echo based sequences less optimal. Combined with a longer  $T_1$ , shorter  $T_2$ ,  $B_0$  and  $B_1^+$  inhomogeneities and SAR restrictions it is a challenging task to obtain a black blood image. In this study different blood suppression techniques that require no or only a small blood preparation slab, are evaluated at 7 tesla by means of a phantom study. The ability to suppress the signal of the blood as well as the effect on the static tissue of the different methods is evaluated. A proof of feasibility was also provided on three healthy volunteers.

**Methods:** All experiments were performed on a Philips 7T with local excitation coils and receive array [1]. All scans were made with an acquisition matrix of 280x280, a FOV of 140x140x2mm, a FA of 30°, TE/TR 4.5ms/1-2s. Only 1 k-line was acquired per TR. Tested methods were *Regional Saturation Technique (REST)*[2], *improved Motion-Sensitized Driven-Equilibrium (iMSDE)*[3], *Phase Sensitive Double Inversion Recovery (PSDIR)* (fig. 2), *Phase Sensitive Single Inversion Recovery (PSSIR)* (fig. 3), *Turbo Spin Echo (TSE)* (turbo factor: 2, start-up echoes: 4), *Stimulated Echo Acquisition Mode (STEAM)* and *Delay alternating with nutation for tailored excitation (DANTE)*[4]. Two methods required post processing: for PSDIR, the complex images of the two acquisitions were summed up, for PSSIR the real part of the second image was used after phase correction. Blood in PSSIR was identified by its reversing polarity between the first and second image, and was set to zero in the phase corrected image.

A flow phantom was created to adjust the flow speed. Quantitative flow measurements were obtained to study the relation between suppression and flow speed. Sensitivity to  $B_1^+$  imperfections in the static tissue was assessed by relating the amount of signal loss in static tissue to the local  $B_1^+$ . A reference image was obtained for each experiment to measure the amount of suppression for the flowing spins compared to signal from the static spins. As TSE has intrinsic black blood properties, the effects on the static tissue were not taken into account for this method. As a proof of principle, single slice images were acquired in three healthy volunteers, using all different blood suppression strategies. All volunteers signed an informed consent, according to the ethical regulations of the institute.

**Results:** Fig. 4 shows examples of the phantom experiments with equal noise scaling. Fig. 5 shows the relative fluid suppression of each method as a function of the flow speed in the phantom. Fig. 6 shows the residual static signal at locations where the  $B_1^+$  was 100%, in the range of 80% to 120%  $B_1^+$  and in the range of 60% - 140%  $B_1^+$ . Figure 3 shows example images of single slice in-vivo experiments.

**Discussion:** Seven different methods to suppress the signal of the blood were tested with local excitation coils. Different methods rely on different mechanisms: saturation (REST), phase reversion (PSDIR, PSSIR), static tissue refocusing (TSE, STEAM) and flow heterogeneity (iMSDE, DANTE). Especially PSDIR, PSSIR, TSE and STEAM produce acceptable blood suppression at 7 tesla. However, signal from the static tissue is also an important factor to consider. PSDIR combines two acquisitions of the signal of the static tissue, increasing the SNR. The loss of signal in case of PSSIR is due to repetitive inversions (saturation), however, a  $T_1$  weighted contrast is achieved, which is a desired contrast for the detection of plaque haemorrhage. A STEAM sequence has an intrinsic loss of a factor 2 of signal. The use of iMSDE introduces  $T_2$ -weighting in the static tissue and produces a varying signal intensities in inhomogeneous  $B_1^+$  fields.

**Conclusion:** In ultra-high field (>7T) MRI, alternative blood suppression techniques are needed to expand the feasibility of different contrast weightings for the carotid artery imaging. In this study different black blood methods have been evaluated. This work compared the different methods so an optimal method can be chosen depending on the required contrast; PSSIR is a convenient method for  $T_1$  weighted images, TSE for  $T_2$  weighted images and PSDIR for PD weighted images.

**References:** (1) Koning et al. *MRM* 2012 (2) Felmlee et al. *Radiology* 1987 (3) Wang et al. *JMRI* 2012 (4) Li et al. *MRM* 2012

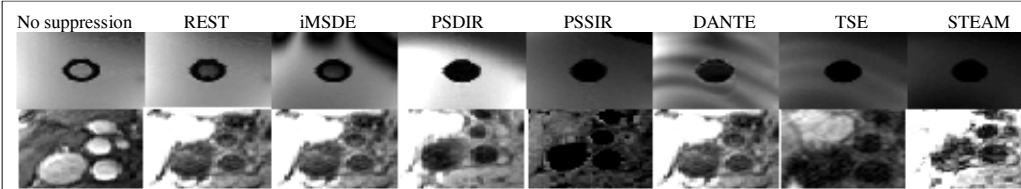


Figure 4: Results of phantom (top row) and in vivo (bottom row) experiments

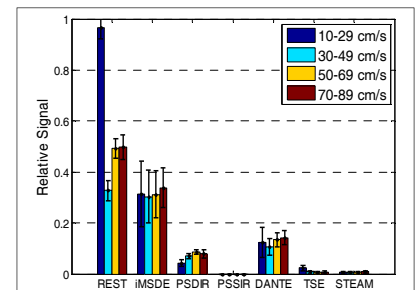


Figure 5: Signal of flowing spins as function of speed

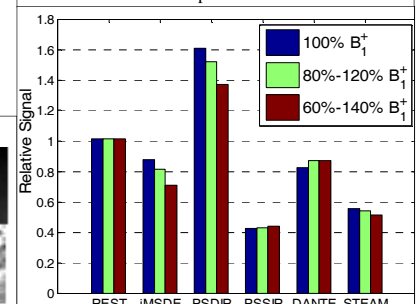


Figure 6: Signal of static spins as function of  $B_1^+$